

## Instability of the Electron Gas in an Expanding Metal

K. Matsuda,<sup>1,\*</sup> K. Tamura,<sup>1</sup> and M. Inui<sup>2</sup>

<sup>1</sup>*Department of Materials Science and Engineering, Kyoto University, Kyoto 606-8501, Japan*

<sup>2</sup>*Faculty of Integrated Arts and Sciences, Hiroshima University, Higashi Hiroshima 739-8521, Japan*

(Received 8 January 2007; published 27 February 2007)

We have measured x-ray diffraction and small-angle x-ray scattering of fluid rubidium by reducing electron density down to the range where the compressibility of the interacting electron gas has been theoretically predicted to become negative. Negative compressibility is closely associated with a negative value of the static dielectric function, which makes the screened Coulomb interaction among like charges overall attractive. It was clearly observed that the interatomic distance decreases in spite of the fact that *mean* interatomic distance increases with expansion, suggesting that an attractive interaction among like charges, ions in this case, is enhanced. These findings indicate that the observed structural features are evidence of the compressional instability of the 3D electron gas.

DOI: [10.1103/PhysRevLett.98.096401](https://doi.org/10.1103/PhysRevLett.98.096401)

PACS numbers: 71.10.Ca, 61.10.-i, 61.25.Mv, 62.50.+p

Since Wigner's pioneering work [1], the anomalous behaviors of low-density electron gas, such as ferromagnetism [2] or superconductors [3,4], has been extensively investigated. The phase behavior of electron gas has been discussed on the basis of ground-state energy, which is conventionally given as a function of the expansion parameter  $r_s$  ( $r_s$  is the Wigner-Seitz radius in units of Bohr radius). To date, quantum Monte Carlo calculations [2] have enabled an essentially accurate determination of ground-state energy and various thermodynamic quantities have been deduced. An intriguing but established property deduced from ground-state energy is compressibility. It becomes negative when  $r_s > 5.25$ , implying the thermodynamic instability of low-density electron gas [2,5,6]. The appearance of the negative compressibility has posed an issue of the possibility that the electron gas undergoes a phase transition resembling an ordinary liquid-gas transition [7,8] or a transition into a broken-symmetry phase such as the Wigner crystal [9].

Negative compressibility is closely associated with the negative sign of the electron static dielectric function (DF),  $\epsilon(\mathbf{q}, 0)$ , at a small  $|\mathbf{q}|$  by taking the compressibility sum rule into account [5]. The negative sign of the static DF of electron gas is theoretically possible without violating any causality or stability requirements, and appears only if the exchange and correlation effects are taken into account [10,11]. In a medium of electron gas with a static negative DF, an unusual situation might be caused in which test charges with the same sign, either positive or negative, attract. Here, a question arises as to whether the negative sign of the static electron DF really exists and is observable in real systems such as metals. Although the existence of the negative electron DF has been reported thus far in a synthesized two-dimensional system such as the interface between semiconductors, the existence of the negative electron DF in a three-dimensional system has never been confirmed [12].

One of the possible means of observing the negative sign of the electron DF is to measure structural properties.

Suppose that positive ions in metals are viewed as test charges put in the electron gas. An attractive Coulomb force appears to work between the ions when the DF of the electron gas becomes negative. Therefore, it would be probable that the static or dynamic structures of ions are changed. In this sense, ions could be a probe for investigating the instability of electron gas. Actually, it has been suggested that the negative sign of the electron DF might lead to lattice instability through the coupling of electrons with the phonon system of the crystal [11]. Also, a similar suggestion was given for the jellium model [13]: if the constraint of a uniform rigid background is eliminated, the condition  $\epsilon(\mathbf{q}, 0) < 0$  brings about a spontaneous density fluctuation of the background with corresponding  $|\mathbf{q}|$ .

Expanded fluid alkali metals [14] are an ideal material for solving the problem of electron gas instability for the following reasons: First, alkali metals are a typical prototype of three-dimensional electron gas. Second, a continuous and substantial reduction in electron density is possible by utilizing volume expansion along the liquid-vapor saturation line. Third, positive ions in fluids can readjust their positions easily compared with those in solids, thus structural change might be more pronounced in fluids through the coupling of electrons and ions.

We have recently devised a sample cell with x-ray windows made of single-crystalline molybdenum resistant to the high reactivity of hot alkali metals [15]. By combining this cell with a high-pressure apparatus [16], we have succeeded in measuring the x-ray diffraction and small-angle x-ray scattering (SAXS) of fluid rubidium over a wide range of temperatures and pressures from the triple point up to supercritical regions. We have obtained structural data using a synchrotron radiation source.

X-ray diffraction analysis was carried out in the energy-dispersive mode at the BL28B2 beam line at SPring-8 in Japan. White x rays were used as the incident beam, and scattered x rays were detected using a pure-germanium solid-state detector. Small-angle x-ray scattering measurement was performed at the BL04B2 beamline at SPring-8.

Monochromatized 38 keV x rays were used as incident beam and scattered x rays were detected using an imaging plate. Stable and precise measurements were carried out for the first time from the triple point up to 2123 K and 22.0 MPa beyond the critical point of rubidium.

The measured structure factor  $S(Q)$  for fluid rubidium is plotted at different temperatures, pressures, and densities in Fig. 1. The  $S(Q)$  data in the low- $Q$  region were obtained

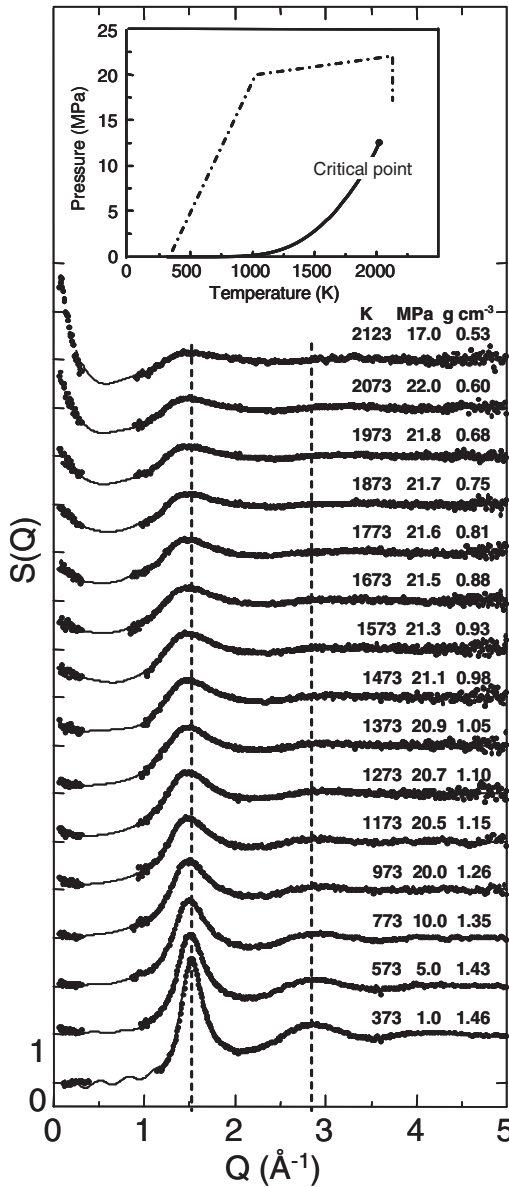


FIG. 1. Structure factors  $S(Q)$  for expanded fluid rubidium at various temperatures and pressures. Temperature, pressure and density are indicated on the upper right-hand side of each data set. The dots represent the experimental data and the full curves show the Fourier transforms of  $g(R)$  in Fig. 2. The broken line indicates the position of the first peak and second one of  $S(Q)$  at 373 K, respectively. The inset shows the phase diagram of rubidium ( $T_c = 2017$  K,  $P_c = 12.45$  MPa) [14] in which dot-and-dash line indicates the path of the conditions at which the present measurements were performed.

by SAXS measurement separately carried out. With increasing temperature (decreasing density), both intensities of the first and second maxima decrease. However, the overall oscillatory structure persists even in the high-temperature region of up to 2123 K. As seen in the figure, the first maximum slightly shifts to a lower  $Q$  with decreasing density. On the contrary, the second peak of  $S(Q)$ , which is not completely blurred out, shifts to a relatively higher  $Q$  region.

The pair distribution function  $g(R)$  is deduced from the Fourier transform of  $S(Q)$  and is shown in Fig. 2. The peak height of the first maximum of  $g(R)$  progressively decreases, whereas that of the second maximum approaches one. Note that the position of the first maximum starts to shift to a low  $R$  below density of  $1.1 \text{ g cm}^{-3}$ .

The density variation of the position of the first maximum,  $R_1$ , is shown in Fig. 3(a).  $R_1$  corresponds to the

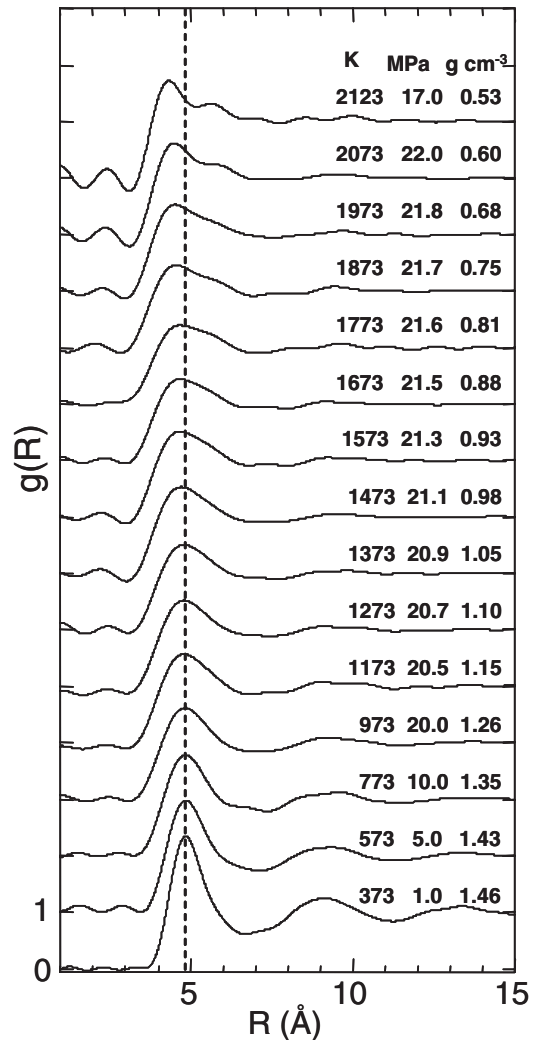


FIG. 2. Pair distribution function  $g(R)$  of expanded fluid rubidium derived from Fourier transform of  $S(Q)$ . The broken line denotes the peak position of the first maximum of  $g(R)$  at 373 K. Temperature, pressure and density are indicated on the upper right-hand side of each curve.

average nearest-neighbor distance. It is located at approximately 4.85 Å at 373 K and is almost the same as that of the solid state. It remains constant with a decreasing density from 1.5 to 1.1 g cm<sup>-3</sup> and then starts to decrease. It gradually decreases with further density decrease and shows saturation at approximately 4.2 Å at densities lower than 0.5 g cm<sup>-3</sup>. Figure 3(b) shows the density variation in coordination numbers which is derived by integrating the radial distribution function defined by  $4\pi R^2 n_0 g(R)$  ( $n_0$ : number density) up to the first-minimum position. The coordination number decreases substantially and almost linearly with decreasing density from 1.5 to 1.1 g cm<sup>-3</sup> and then shows a strong deviation from a linear dependence, remaining at approximately 6 until reaching 0.7 g cm<sup>-3</sup>.

The structural change observed in the density range from 1.1 to 0.5 g cm<sup>-3</sup> is quite opposite to that expected because interatomic distance decreases despite mean interatomic distance increasing with volume expansion. The present results on  $R_1$  are, in fact, completely opposite to those previously obtained by the neutron diffraction measurements [17] in which  $R_1$  rather increased with decreasing density. These structural features strongly indicate that an

attractive force appears to work among ions in the density range from 1.1 to 0.5 g cm<sup>-3</sup>. Note that the coordination number shows a deviation from a linear decrease and is maintained constant in the range from 1.1 to 0.7 g cm<sup>-3</sup> in spite of progressive expansion, which indicates the appearance of a spatial inhomogeneity.

It is critical that local structural parameters (i.e., interatomic distance and coordination number) be scaled by the expansion parameter  $r_s$ . In real metals, the effect of core polarization by ions reduces the strength of the effective interaction among electrons. Kukkonen *et al.* [18] pointed out that an ionic background can be viewed as a uniform and polarizable background by taking core polarizability to be a constant. Thus,  $r_s$  for the electron gas in metals should be scaled with  $r_s^* = r_s/\epsilon_b$  rather than with  $r_s$ , where  $\epsilon_b$  is the dielectric constant of the polarizable background defined by  $\epsilon_b = 1 + 4\pi n\alpha$  ( $\alpha$ : ionic polarizability,  $n$ : the number density of ions). This corrected  $r_s$  ( $= r_s^*$ ) is shown on the upper horizontal axis of Fig. 3(a). As seen in the figure,  $R_1$  starts to decrease and the coordination number shows a deviation from a linear decrease between  $r_s^* = 5$  and 5.5. This density range agrees well with the critical  $r_s$  ( $= 5.25$ ) beyond which the compressibility of electron gas becomes negative and also the static electron DF becomes negative at a low wave vector. The negative electron DF generates an attractive Coulomb interaction among test charges with the same sign—the charges of ions in this case. The observed local contraction in the metallic state below 1.1 g cm<sup>-3</sup> can be interpreted as structural variation caused by the enhancement in the attractive force among the ions. The local contraction indicates an increase in local atomic density, which would generate a rare region of density at the same time.

Such inhomogeneous structure was also observed in our SAXS measurement. As shown in Fig. 1, the  $S(Q)$  at a low  $Q$  less than 0.3 Å<sup>-1</sup> starts to increase with decreasing  $Q$ , which indicates the appearance of density fluctuation. We derived correlation length  $\xi$  and  $S(0)$  using the Ornstein-Zernike formula. Fig. 4(a) shows density dependence of the correlation length for expanded fluid rubidium. The correlation length is about 5 Å around 1.2 g cm<sup>-3</sup> and remains almost constant around it in the density range from 1.2 to 0.6 g cm<sup>-3</sup>, which corresponds to the density range where the appearance of structural inhomogeneity was suggested in our x-ray diffraction analysis. Then it substantially increases below 0.6 g cm<sup>-3</sup> as the density of the fluid approaches  $\rho_c$ . Figure 4(b) shows density dependence of  $S(0)$  for expanded fluid rubidium.  $S(0)$  gradually increases with decreasing density and is observable in the density range from 1.1 to 0.6 g cm<sup>-3</sup>. Then it shows a substantial increase below 0.6 g cm<sup>-3</sup> as the fluid density approaches the critical one.

In addition to the measurement up to the critical region, we measured SAXS at thermodynamic conditions far from the critical point. Density dependence of  $\xi$  and  $S(0)$  at constant pressure of 5 MPa, which is lower than  $P_c$ , is also

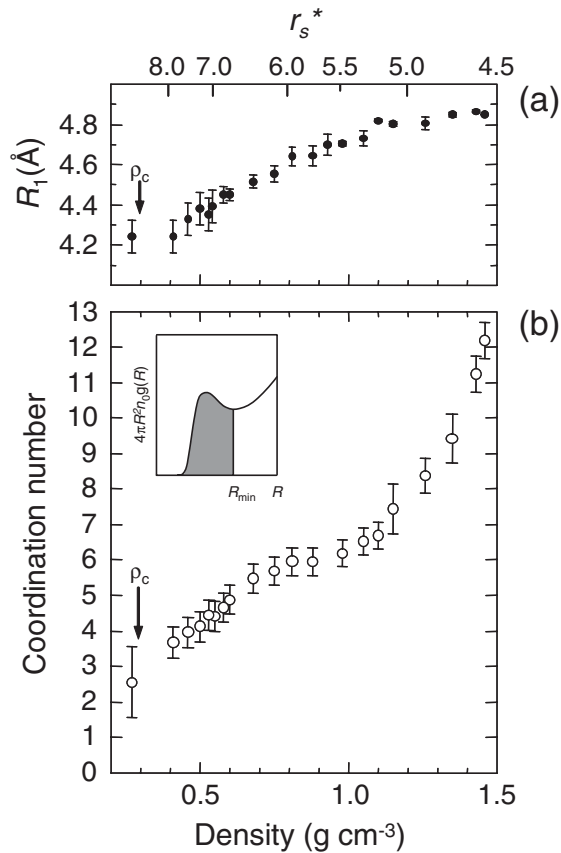


FIG. 3. Density dependence of local structure of fluid rubidium. (a) Density dependence of interatomic distance  $R_1$ . (b) Density dependence of coordination number. The critical density is denoted  $\rho_c$ . The corresponding scale of  $r_s^*$  is shown on the upper axis of the graph of  $R_1$ .

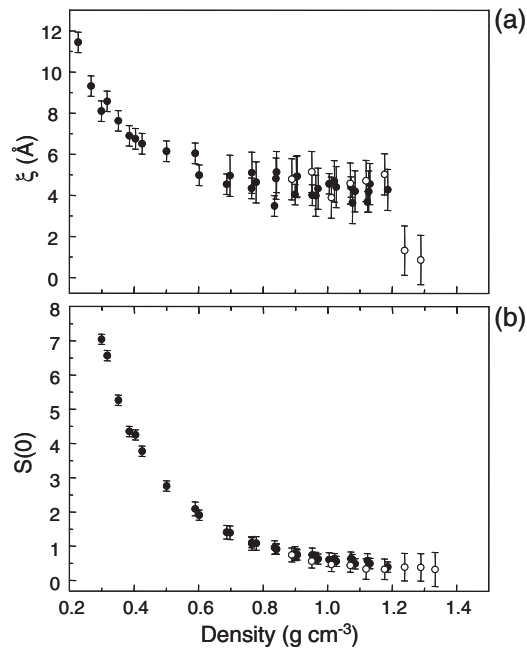


FIG. 4. Density dependence of correlation length and  $S(0)$  for expanded fluid rubidium up to the critical region. Dots represent the data measured at the conditions as shown in the inset in Fig. 1. Open circles indicates the data measured at the pressure of 5 MPa.

shown as open circles in Fig. 4. Even far from the critical point, the increase in  $S(0)$  was observed in the metallic liquid range (0.9–1.1 g cm<sup>-3</sup>) where the measurement was carried out, which might indicate that density fluctuation around this range is not interpreted as a tail of the critical one but is attributed to the fluctuation intrinsic to phase behaviors of the electronic system. According to Pines and Nozieres [13], the negative static DF of the electronic system brings about a spontaneous density fluctuation of the background if the constraint of a uniform rigid background is eliminated. In the fluid system, the ions can rearrange their positions easily compared with those in solids. Therefore, the density fluctuation in the range from 1.1 to 0.6 g cm<sup>-3</sup> might be related to the electron gas instability, i.e., the negative DF of the electron gas.

Theoretical efforts have been made to understand the physical meaning of the negative DF of electron gas from the microscopic point of view [19,20]. The negative sign of the static electron DF has been considered to be responsible for an attractive Coulomb interaction among electrons, when electrons are regarded as test charges, which raises the possibility of electron pairing. Various theories have predicted that the negative static DF is closely associated with the appearance of superconductivity [11,21–23]. We could not rule out the possibility that expanded fluid alkali metals become superconducting state at low temperatures if their structural response to the

negative electron DF could be frozen as in the doped cuprates [24].

The authors are grateful to Professor Y. Takada for helpful discussion and comments. The authors also thank M. Katoh of Allied Materials Corp. and K. Kato and S. Kohara of SPring-8. The synchrotron radiation experiments were performed at the SPring-8 with the approval of the Japan Synchrotron Radiation Research Institute (JASRI). This work was supported by Grant-in-Aid for Scientific Research Fund from the Ministry of Education, Culture, Sports, Science and Technology (Research No. 11102004 and No. 16760532).

\*Electronic address: kazuhiko-matsuda@mtl.kyoto-u.ac.jp

- [1] E. P. Wigner, Phys. Rev. **46**, 1002 (1934).
- [2] D. M. Ceperley and B. J. Alder, Phys. Rev. Lett. **45**, 566 (1980).
- [3] W. Kohn and J. M. Luttinger, Phys. Rev. Lett. **15**, 524 (1965).
- [4] Y. Takada, Phys. Rev. B **39**, 11 575 (1989).
- [5] G. Giuliani and G. Vignale, *Quantum Theory of the Electron Liquid* (Cambridge University Press, Cambridge, England, 2005).
- [6] G. D. Mahan, *Many-Particle Physics* (Kluwer Academic/Plenum, New York, 2000).
- [7] N. Wiser and M. H. Cohen, J. Phys. C **2**, 193 (1969).
- [8] M. D. Llano and V. V. Tolmachev, Phys. Lett. B **37**, 37 (1971).
- [9] C. M. Care and N. H. March, Adv. Phys. **24**, 101 (1975).
- [10] O. V. Dolgov, D. A. Kirzhnits, and E. G. Maksimov, Rev. Mod. Phys. **53**, 81 (1981).
- [11] O. V. Dolgov and E. G. Maksimov, Sov. Phys. Usp. **25**, 688 (1982).
- [12] J. P. Eisenstein, L. N. Pfeiffer, and K. W. West, Phys. Rev. Lett. **68**, 674 (1992).
- [13] D. Pines and P. Nozieres, *The theory of Quantum Liquids* (W. A. Benjamin, inc., New York, 1966), Vol. 1.
- [14] F. Hensel and W. W. Warren, Jr., *Fluid Metals: The Liquid-Vapor Transition of Metals* (Princeton University, Princeton, NJ, 1999).
- [15] K. Matsuda, K. Tamura, M. Katoh, and M. Inui, Rev. Sci. Instrum. **75**, 709 (2004).
- [16] K. Tamura and M. Inui, J. Phys. Condens. Matter **13**, R337 (2001).
- [17] G. Franz, W. Freyland, W. Glaser, F. Hensel, and E. Schneider, J. Phys. (Paris), Colloq. **8**, 194 (1980).
- [18] C. A. Kukkonen and J. W. Wilkins, Phys. Rev. B **19**, 6075 (1979).
- [19] Y. Takada, J. Supercond. **18**, 185 (2005).
- [20] K. Takayanagi and E. Lipparini, Phys. Rev. B **56**, 4872 (1997).
- [21] A. Bagchi, Phys. Rev. **178**, 707 (1969).
- [22] D. R. Penn, S. P. Lewis, and M. L. Cohen, Phys. Rev. B **51**, 6500 (1995).
- [23] M. Tachiki, Phys. Rev. B **67**, 174506 (2003).
- [24] P. Quemerais, J.-L. Raimbault, and S. Fratini, J. Phys. IV **12**, 227 (2002).